Li local configurations for the trimerized state of the geometrically frustrated triangular lattice system $Li_{1-x}V O_2$ with $0 \leq x \leq 0.14$

2010 J. Phys.: Condens. Matter 22 116003

(http://iopscience.iop.org/0953-8984/22/11/116003)

J. Phys.: Condens. Matter **22** (2010) 116003 (6pp) doi:10.1088/0953-8984/22/11/116003

Li local configurations for the trimerized state of the geometrically frustrated triangular lattice system $Li_{1-x}VO_2$ with $0 \leqslant x \leqslant 0.14$

Kenjiro Takao and Masashige Onoda

Institute of Physics, University of Tsukuba, Tennodai, Tsukuba 305-8571, Japan

E-mail: onoda.masashige.ft@u.tsukuba.ac.jp

Received 18 December 2009, in final form 28 January 2010
Published 23 February 2010
Online at stacks.iop.org/JPhysCM/22/116003

Abstract
The Li de-intercalation effects for the trimerized state of the geometrically frustrated triangular lattice $LiVO_2$ are investigated through measurements of x-ray diffraction, magnetic susceptibility and magic-angle spinning-nuclear magnetic resonance (MAS-NMR). $Li_{1-x}VO_2$ with $0 \leqslant x \leqslant 0.14$ obtained with a soft-chemistry synthesis is a single phase. All of the data are understood by considering that the partial substitution for V^{3+} (spin-1) with V^{4+} (spin-$\frac{1}{2}$) leads to the coexistence of the spin-singlet and spin-$\frac{1}{2}$ trimers.

1. Introduction

Layered oxide systems with a chemical formula $M_{1-x}TO_2$, M and T being alkaline and transition-metal atoms, respectively, have been explored extensively from various viewpoints. Basic physics on the geometrically frustrated triangular lattice system has been studied for a long time, including superconductivity in the hydrated $Na_{0.3}CoO_2{\cdot}1.3H_2O$ [1]. Applied sciences such as rechargeable batteries for M = Li and T = Co or Ni [2–4], and thermoelectric devices for M = Na and T = Co [5], have also received considerable attention.

$LiVO_2$ basically has an ordered rocksalt structure with a space group of $R\bar{3}m$, where each ion occupies alternating (1 1 1) cubic planes. V^{3+} ions with spin-1 form a two-dimensional triangular lattice with antiferromagnetic exchange couplings, leading to a geometrical spin frustration. This compound undergoes a first-order magnetic to nonmagnetic phase transition at T_c = 440–500 K [6, 7]. Below T_c, the electrical conductivity exhibits a rapid decrease and the superlattice reflections with ($\frac{1}{3}$ $\frac{1}{3}$ 0) appear [7, 8]. For a mechanism of this phase transition, the formation of triangular vanadium clusters or trimers at temperatures below T_c was suggested [9]. Here, V ions slightly shift to the center of a triangle from a regular triangular lattice as shown in figure 1. Then, considering a set of isolated trimers with the Hamiltonian

$$H = J(\boldsymbol{S}_1 \cdot \boldsymbol{S}_2 + \boldsymbol{S}_2 \cdot \boldsymbol{S}_3 + \boldsymbol{S}_3 \cdot \boldsymbol{S}_1), \tag{1}$$

where J is the exchange coupling constant and $\boldsymbol{S}_i$ (i = 1–3) is the spin-1 operator, the experimental results were explained [7, 10–12]. This spin-singlet trimerization is partly supported from the viewpoint of the orbital ordering [13]. Here, it should be noted that the trimerized state may be incoherent for the direction normal to the basal plane. In addition, a small doping of spin-$\frac{3}{2}$ and 0 for this system leads to spin-$\frac{1}{2}$ and 0 per three V ions as a ground state, respectively [14], and that of spin-$\frac{1}{2}$ in $Na_{0.7}VO_2$, which has a structure similar to $LiVO_2$, also leads to a spin-$\frac{1}{2}$ trimer [12]. Moreover, the pseudotrimer model obtained with a constant coupling approximation for interactions between the triangular clusters expressed by equation (1) explains successfully the paramagnetic state for the frustrated triangular lattice system [12].

The synthesis of $Li_{1-x}VO_2$ and its structural model were reported previously [15–25], but there is no systematic investigation of the physical properties. The single crystals (x = 0.2–0.3) prepared by fused-salt electrolytic or flux methods show superlattice reflections with ($\frac{1}{3}$ $\frac{1}{3}$ $\frac{1}{4}$), in addition to the case of $LiVO_2$ [11, 18, 22]. It is not easy to control the Li concentration for these crystals. For the polycrystals, on the

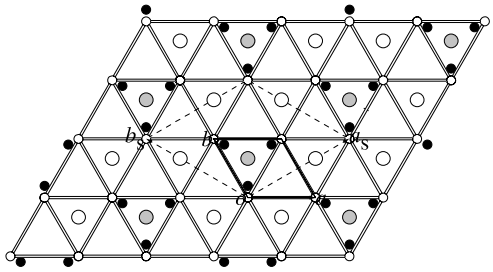

Figure 1. The schematic view of trimerization in the basal plane of $LiVO_2$ at temperatures below T_c. Here, the small open circles denote the V positions ($z = 0$) in the average cell expressed by the full lines, while the small full circles indicate the possible displacement pattern of V in the superlattice cell shown by the dashed lines. The large open and shaded circles are the α and β positions of Li ($z = 1/6$), respectively.

other hand, the Li concentration can be varied in terms of the chemical or electrochemical methods [15]. Depending on the Li concentration, two kinds of rhombohedral phase appear; R1 phase with $0 \leqslant x \leqslant 0.3$ and R2 phase with $0.7 < x \leqslant 0.9$. For the intermediate concentration, the system has a mixed phase of R1 and R2 [15]. For a certain x, an irreversible transition to the spinel phase of LiV_2O_4 occurs at about 520 K [16].

This work is performed to clarify systematically the structural, magnetic and microscopic properties of the R1 phase in $Li_{1-x}VO_2$ prepared soft-chemically. The details regarding the sample preparation and the measurements are written in section 2. The results of structural aspects and magnetic susceptibilities are discussed in sections 3.1 and 3.2, respectively. The microscopic properties revealed by magic-angle spinning-nuclear magnetic resonance (MAS-NMR) for ^{51}V and ^{7}Li nuclei are presented in section 3.3. Section 4 is devoted to conclusions.

2. Experiments

Polycrystalline specimens of $LiVO_2$ were prepared by the solid-state reaction method [7, 14]. The Li ions were extracted soft-chemically from $LiVO_2$ using Br_2/CH_3CN solution [15]. Inductively coupled plasma-optical emission spectroscopy (ICP) was performed using a Nippon Jarrell-Ash ICAP-757 spectrometer. An x-ray powder diffraction pattern was taken with Cu Kα radiation using a Rigaku RAD-IIC diffractometer. The magnetization measurements were performed by the Faraday method with a field of up to 1 T. The magnetic susceptibility was deduced from the linear part of the magnetization field (M–H) curve with a decreasing field. The MAS-NMR spectra were recorded on a Bruker Avance 600 at 233.23 MHz for ^{7}Li and at 157.79 MHz for ^{51}V at room temperature. The external fields were calibrated by an LiCl solution for ^{7}Li spectra.

3. Results and discussions

3.1. Structural aspects

The x-ray powder diffraction patterns and ICP analysis indicate compounds with $0 \leqslant x \leqslant 0.14$ to be single phase. For the

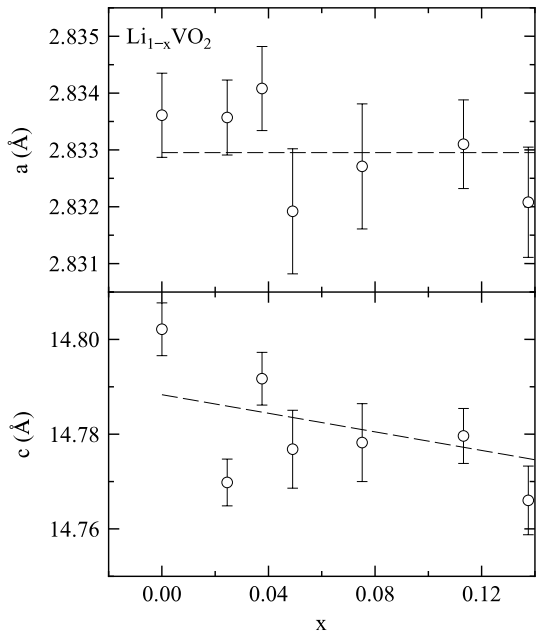

Figure 2. The composition dependences of lattice constants for the average structure of $Li_{1-x}VO_2$, where the dashed lines are a guide for the eyes.

range of $0.14 < x < 0.66$, the compounds are a mixed phase of R1 and R2. These results are qualitatively consistent with the previous report [15]. In addition, the Li de-intercalated system decomposes into the spinel-type LiV_2O_4 phase with the space group $Fd\bar{3}m$ at temperatures above 500 K [16].

The superlattice reflections with $(\frac{1}{3}\ \frac{1}{3}\ 0)$, suggesting the trimerized atomic displacements shown in figure 1, are observed for all of the compositions. The lattice constants of the average structure against x are shown in figure 2. While a does not change on x, c decreases with increasing x. Figure 3 shows the x dependences of integrated intensities of $(\frac{1}{3}\ \frac{1}{3}\ 0)$ reflections normalized with those of (0 0 3), which do not depend significantly on x. These results suggest that the trimerized states are stable for the small amount of Li de-intercalation.

3.2. Magnetic susceptibilities

The temperature dependences of inverse magnetic susceptibilities for $Li_{1-x}VO_2$ are shown in figure 4. For all of the compositions, the data are fitted with the Curie–Weiss law:

$$\chi = C/(T + T_W) + \chi_0, \tag{2}$$

where C is the Curie constant, T_W is the Weiss temperature and χ_0 is the temperature-independent susceptibility from the orbital paramagnetism and diamagnetism. The full curves in figure 4 provide the Curie constants as a function of x shown in figure 5, where T_W and χ_0 are of the order of 10^0 K and 10^{-5} emu mol^{-1}, respectively.

The temperature-dependent susceptibility of the end-member $LiVO_2$ is a contribution from impurity spins and/or lattice imperfections, since in this composition the spin-singlet trimerized state is formed. Here, the impurity concentration is

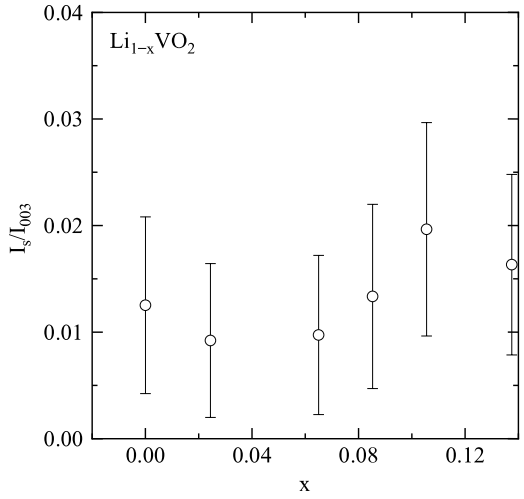

Figure 3. The composition dependences of integrated intensities of $(\frac{1}{3}\ \frac{1}{3}\ 0)$ reflections normalized with those of (0 0 3) in $Li_{1-x}VO_2$.

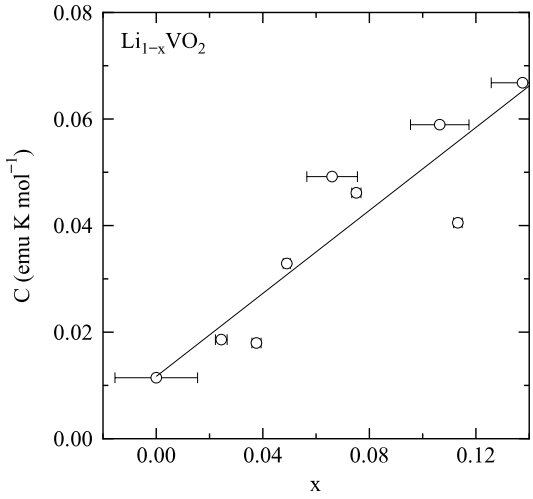

Figure 5. The composition dependences of Curie constants of $Li_{1-x}VO_2$, where the full line indicates the relation given in the text.

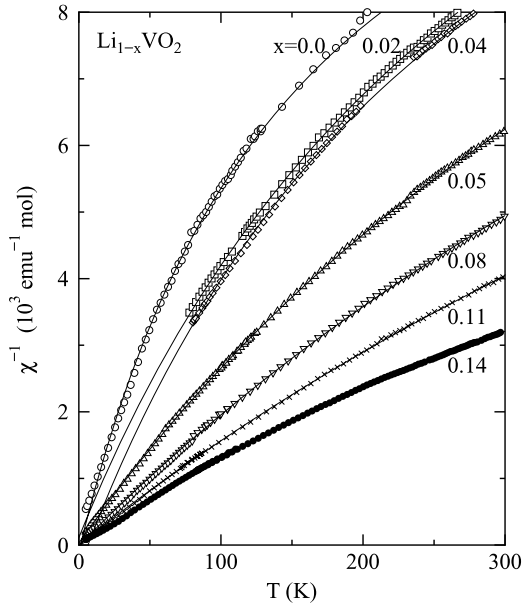

Figure 4. The temperature dependences of inverse magnetic susceptibilities of $Li_{1-x}VO_2$, where the full curves are the results calculated from equation (2) with parameters presented in figure 5 and the text.

3% per chemical formula with the assumption of $g = 2$ and spin-$\frac{1}{2}$.

Let us consider that the Li de-intercalated system also exhibits a structural distortion similar to that of $LiVO_2$ as suggested in section 3.1. The x Li de-intercalated system should have the average valence $V^{(3+x)+}$ from the ionic state of $(1-x)V^{3+}$ and xV^{4+}. For the small Li de-intercalation, it is sufficient to consider the local triangular cluster with two spin-1 and one spin-$\frac{1}{2}$. In this case, the ground state of the local trimer is spin-$\frac{1}{2}$ and the spin susceptibility is written as [12]

$$\chi_{\mathrm{d}}^{t'} = \frac{3}{19}\frac{C}{T}\frac{2+20p^{3/2}+35p^4}{2+4p^{3/2}+3p^4}, \tag{3}$$

where C and p are the Curie constant and $\exp(-J/T)$, respectively, J being the exchange coupling constant. At temperatures lower than J, equation (3) approximately provides the Curie law expressed as

$$\chi_{\mathrm{d}}^{t'} = \frac{N_{\mathrm{A}}g^2\mu_{\mathrm{B}}^2}{12k_{\mathrm{B}}T}, \tag{4}$$

where N_{A} is Avogadro's number, μ_{B} is the Bohr magneton and k_{B} is the Boltzmann constant. Thus, the composition dependence of C for the small Li de-intercalation is written as $C = 0.375x$ for $g = 2$. In effect, the full line for the Curie constants against x shown in figure 5 provides $C = 0.012(5) + 0.39(6)x$, which indicates that the local trimer model is valid for the present system.

The transitions to the fully paramagnetic states with increasing temperature are observed. The transition temperatures seem to depend little on x:$T_{\mathrm{c}} = 530 \pm 10$ K, although precise determinations of T_{c} are difficult for the Li de-intercalated system owing to the phase separation near T_{c}. This result may be consistent with the near independence of lattice constant a on x. In other words, the exchange coupling constants in this system do not change x significantly. On the other hand, in $Li_{1-x}Mg_xVO_2$ and $LiV_{1-x}Al_xO_2$, it is known that, with increasing x, T_{c} decreases and a increases: for $Li_{0.94}Mg_{0.06}VO_2$, $T_{\mathrm{c}} = 410$–470 K and $a = 2.842$ Å; and for $LiV_{0.9}Al_{0.1}O_2$, $T_{\mathrm{c}} = 400$–450 K and $a = 2.844$ Å [14].

3.3. MAS-NMR for ^{51}V and ^{7}Li nuclei

The ^{51}V MAS-NMR spectra of $Li_{1-x}VO_2$ ($x = 0$ and 0.12) at room temperature are shown in figure 6(a). The weighted center of the spectrum for $x = 0$ is about 3180 ppm, which nearly agrees with the previous result $K^{\mathrm{is}} = 0.33(1)$ and $K^{\mathrm{an}} = -0.12(2)\%$ for the orbital paramagnetism on the assumption that the principal axes of the electric field gradient and the Knight shift tensor correspond to each other and that the anisotropy of K is expressed as $K = K^{\mathrm{is}} + K^{\mathrm{an}}(3\cos^2\theta - 1)$, θ being the polar angle of the external

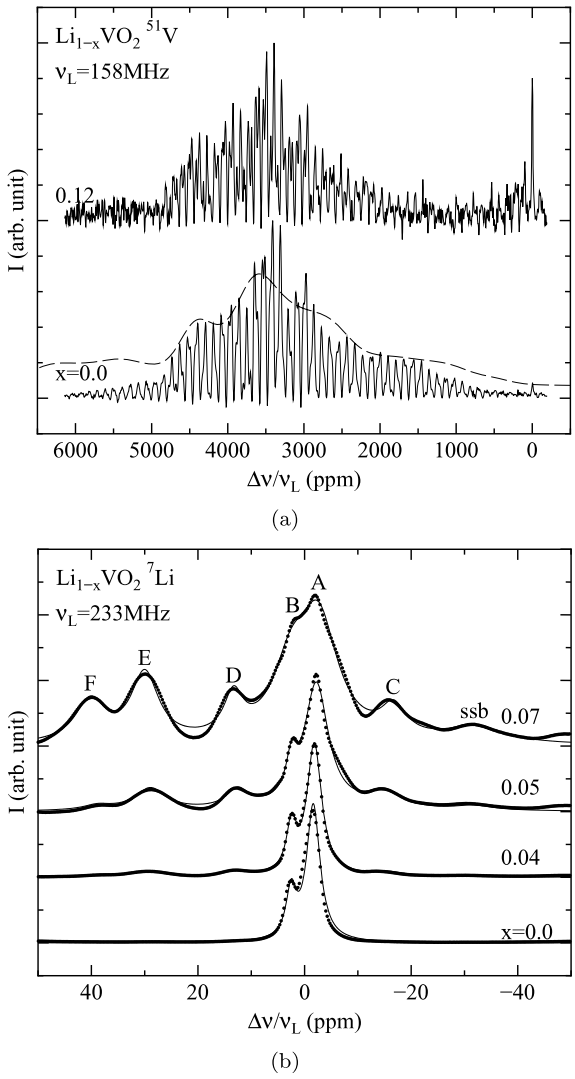

Figure 6. The MAS-NMR spectra of $Li_{1-x}VO_2$ at room temperature: (a) ^{51}V spectra at 157.79 MHz with spinning speeds of 14 kHz; and (b) ^{7}Li central spectra at 233.23 MHz with spinning speeds of 14 kHz. Here, the dashed curve in (a) indicates the spectra calculated on the basis of the previous results for the Knight shifts and nuclear quadrupole interaction parameters [7]. The full curves in (b) indicate fits by the multiple Lorentzians labeled 'A'–'F' and the line labeled 'ssb' is attributed to the spinning side-bands from the E line.

field to the principal axis [7]. The spectra calculated with the above Knight shifts and nuclear quadrupole interaction parameters of $\nu_Q = 0.47$ MHz and $\eta = 0.4$ [7] account for the result as indicated by the dashed curve in figure 6(a). Here, the large width of the spectra is due to the second-order quadrupole effect and the anisotropy of Knight shifts for the orbital paramagnetism. The spectra with $x = 0.12$ are basically similar to those with $x = 0$. This means that a major part of the spin-singlet trimerized state in $LiVO_2$ still remains in the Li de-intercalated system. In addition, the signal with nearly zero shift appears, which may be originated from the spin-$\frac{1}{2}$ trimers having V^{4+} doped by Li de-intercalation.

The ^{7}Li MAS-NMR spectra are shown in figure 6(b). For $x = 0$, only two lines labeled A and B are observed, while for $x \neq 0$, new lines labeled C–F appear additionally

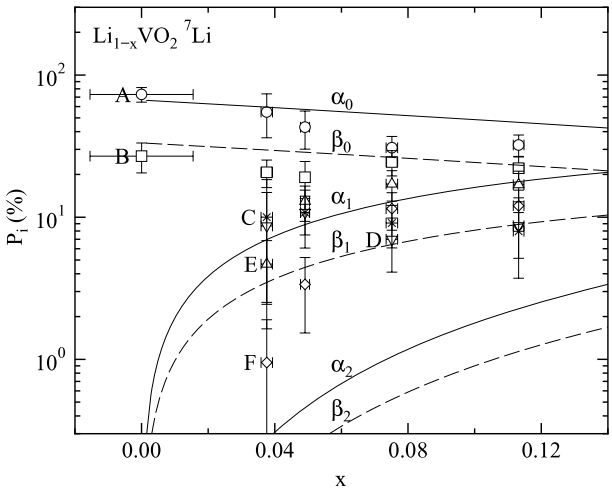

Figure 7. The x dependences of relative intensities of the lines defined in the ^{7}Li MAS-NMR spectra of $Li_{1-x}VO_2$, where the curves are results calculated from equations (5) and (6).

and their intensities increase with increasing x, as shown in figure 7. Generally, for the nuclei with a significant quadrupole interaction, multiple lines in MAS-NMR are often observed. However, this is not the case, since an Li de-intercalation does not change the main lines of $LiVO_2$ but it gives new lines. Therefore, the lines may come from the structural distortion due to the trimerization.

First of all, let us discuss the result for $LiVO_2$. Since the trimerized state may be incoherent for the direction normal to the basal plane [10], the $c/3$ cell for the V and Li layers is considered as the simplest case. As shown in figure 1, there exist two Li sites at $z = \frac{1}{6}$: one α site does not have a trimer at $z = 0$ and another β site has a trimer. Here, the ratio of α to β occupancies is 2:1. This ratio agrees well with the relative intensities estimated from the MAS-NMR spectra.

Next, the origin of additional lines in the Li de-intercalated system is considered. For $x = 0.07$, six lines labeled A–F are assigned as seen in figure 6(b). When V^{4+} ions exist in the V cluster, the α and β sites of Li defined above are separated, depending on the number of V^{4+} in the cluster. That is, there appear eight configurations: α_i and β_i with $i = 0$, 1, 2 and 3, the subscript being the number of V^{4+} in the V cluster. The x dependences of α_i and β_i are described as follows:

$$\alpha_0 = \tfrac{2}{3}(1-x)^3, \qquad \alpha_1 = 2x(1-x)^2,$$
$$\alpha_2 = 2x^2(1-x), \qquad \alpha_3 = \tfrac{2}{3}x^3, \tag{5}$$

$$\beta_i = \tfrac{1}{2}\alpha_i. \tag{6}$$

Since the magnitudes of α_3 and β_3, corresponding to the absence of V^{3+} in the cluster, are very small for the single-phase range of $x \leqslant 0.14$, six lines should appear, which seems to explain the experimental results. The comparison between the experimental and calculated ratios is shown in figure 7. The calculated curves roughly account for the results. The relation between the lines for $x = 0.07$ and the Li local configurations is listed in table 1. As described above, the shift of each line does not depend significantly on x.

Table 1. The relation between the ^{7}Li MAS-NMR spectra and the Li local configurations of $Li_{0.93}VO_2$ at room temperature.

Line	Shift (ppm)	Relative intensity (%)	Li configuration
A	−2	31(6)	α_0
D	12	7(3)	α_1
C	−16	9(3)	α_2
B	2	24(5)	β_0
E	30	17(4)	β_1
F	40	12(3)	β_2

$LiVO_2$ has the α_0 site with a shift of −2 ppm and the β_0 site with 2 ppm. Since the V ions at room temperature are spin-singlets and the magnetic susceptibility comes from the orbital paramagnetism and diamagnetism, the resonance shifts through the transferred hyperfine field are negligibly small.

Due to the Li de-intercalation, that is, the increase of V^{4+} ions, the lines with relatively large shifts appear. This may be attributed to the transferred field from the spin-$\frac{1}{2}$ ground state. In order to understand each resonance shift for $x \neq 0$ qualitatively, we introduce the radial wavefunction of $\psi \sim \exp(-\xi r)$ for d-electrons of V^{4+}, where ξ is a constant, assuming that only V^{4+} ions give the significant transferred hyperfine field. Figure 8 indicates the histogram of the electron transfer from V^{4+} distributed randomly for the α and β sites with the V displacement condition of $\xi = 5/a$ and $\delta/a = 0.05$, δ and a being the shift from the V positions in the average cell and the average V–V distance, respectively (see figure 1). In this condition, the resonance shifts and the relative intensities for A–E are explained roughly with the Li configuration listed in table 1, although the reason why the C-line provides negative shifts is not clear. It should also be noted that, in spite of a rather simple model, the present analysis leads to the V displacement suggested from EXAFS measurements [24].

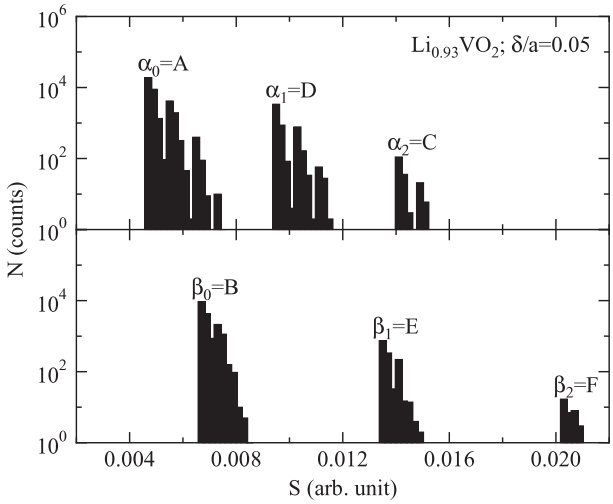

Figure 8. The histogram for the transferred fields from V^{4+} distributed randomly or the resonance shifts S in $Li_{0.93}VO_2$.

4. Conclusions

The structural, magnetic and microscopic properties of the geometrically frustrated triangular lattice system $Li_{1-x}VO_2$ with $0 \leqslant x \leqslant 0.14$ prepared soft-chemically are explored through various measurements of the x-ray diffraction, magnetic susceptibility and MAS-NMR for ^{51}V and ^{7}Li.

The x-ray powder diffraction suggests that the trimerized lattice is still stable for the present Li de-intercalated range. The magnetic susceptibility results are quantitatively explained by the spin-$\frac{1}{2}$ trimer induced by the partial substitution of V^{3+} with V^{4+}. This substitution effect leads to the ^{51}V MAS-NMR signal with a nearly zero shift in addition to the signal similar to that of $LiVO_2$. That is, the Li de-intercalated system is considered as being mixed states of spin-singlet and spin-$\frac{1}{2}$ trimers.

The ^{7}Li MAS-NMR spectra of $LiVO_2$ are explained considering the $c/3$ cell for the V and Li layers. Six magnetically different Li sites for the Li de-intercalated system are also understood using this $c/3$ cell with transferred hyperfine fields from paramagnetic V^{4+} ions. The MAS-NMR measurement is very useful as the sensitive detection of the change of Li local configurations due to the trimerization.

References

[1] Takada K, Sakurai H, Takayama-Muromachi E, Izumi F, Dilanian R A and Sasaki T 2003 *Nature* **422** 53
[2] Mizushima K, Jones P C, Wiseman P J and Goodenough J B 1980 *Mater. Res. Bull.* **15** 783
[3] Dahn J R, von Sacken U and Michal C A 1990 *Solid State Ion.* **44** 87
[4] Kanno R, Kubo H, Kawamoto Y, Kamiyama T, Izumi F, Takeda Y and Takano M 1994 *Solid State Chem.* **110** 216
[5] Terasaki I, Sasago Y and Uchinokura K 1997 *Phys. Rev.* B **56** R12685
[6] Goodenough J B 1963 *Magnetism and the Chemical Bond* (New York: Interscience and Wiley)
[7] Onoda M, Naka T and Nagasawa H 1991 *J. Phys. Soc. Japan* **60** 2550
[8] Tain W, Chisholm M F, Khalifah P G, Jin R, Sales B C, Nagler S E and Mandrus D 2004 *Mater. Res. Bull.* **39** 1319
[9] Goodenough J B, Dutta G and Manthiram A 1991 *Phys. Rev.* B **43** 10170
[10] Onoda M and Inabe T 1993 *J. Phys. Soc. Japan* **62** 2216
[11] See, for review Onoda M and Nagasawa H 1994 *Butsuri (Bull. Phys. Soc. Japan)* **49** 559 (in Japanese)
[12] Onoda M 2008 *J. Phys.: Condens. Matter* **20** 145205
[13] Pen H F, van den Brink J, Khomskii D I and Sawatzky G A 1997 *Phys. Rev. Lett.* **78** 1323
[14] Naka T, Onoda M and Nagasawa H 1993 *Solid State Commun.* **87** 679
[15] de Picciotto L A, Thacheray M M, David W I F, Bruce P G and Goodenough J B 1984 *Mater. Res. Bull.* **19** 1497
[16] de Picciotto L A and Thacheray M M 1985 *Mater. Res. Bull.* **20** 187
[17] de Picciotto L A and Thacheray M M 1985 *Mater. Res. Bull.* **20** 1409
[18] Hewston T A and Chamberland B L 1985 *J. Solid State Chem.* **59** 168
[19] Hewston T A and Chamberland B L 1986 *J. Solid State Chem.* **65** 100

[20] Thacheray M M, de Picciotto L A, David W I F, Bruce P G and Goodenough J B 1987 *J. Solid State Chem.* **67** 285
[21] Cardoso L P, Cox D E, Hewston T A and Chamberland B L 1988 *J. Solid State Chem.* **72** 234
[22] Takei H, Koike M, Imai K, Sawa H, Kadowaki H and Iye Y 1992 *Mater. Res. Bull.* **27** 555
[23] Imai K, Koike M, Sawa H and Takei H 1993 *J. Solid State Chem.* **102** 277
[24] Imai K, Sawa H, Koike M, Hasegawa M and Takei H 1995 *J. Solid State Chem.* **114** 184
[25] Ozawa K, Nakao Y, Wang L, Cheng Z, Fujii H, Hase M and Eguchi M 2007 *J. Power Sources* **174** 469